Neutron-Diffraction Evidence for the Ferrimagnetic Ground State of a Molecule-Based Magnet with Weakly Coupled Sublattices

Randy S. Fishman[1], Javier Campo[2], Thomas E. Vos[3], and Joel S. Miller[3]
[1]*Materials Science and Technology Division, Oak Ridge National Laboratory, Oak Ridge, Tennessee 37831-6071*
[2]*Materials Science Institute of Aragón (CSIC - University of Zaragoza), C/Pedro Cerbuna 12, 50009 Zaragoza, Spain and*
[3]*Department of Chemistry, University of Utah, Salt Lake City, Utah 84112-0850*
(Dated: October 18, 2012)

The diruthenium compound $[Ru_2(O_2CMe)_4]_3[Cr(CN)_6]$ contains two weakly coupled, ferrimagnetically ordered sublattices occupying the same volume. Due to the weak, antiferromagnetic dipolar interaction $K_c \approx 5 \times 10^{-3}$ meV between sublattices, a small magnetic field $H_c \sim K_c/\mu_B \approx 800$ Oe aligns the sublattice moments. Powder neutron-diffraction measurements on a deuterated sample confirms an earlier prediction that the sublattice moments are restricted by the anisotropy of the diruthenium "paddle-wheels" to the cubic diagonals. Those measurements also suggest that quantum corrections to the ground state are significant.

With two weakly interacting and ferrimagnetically ordered sublattices occupying the same volume, diruthenium tetracarboxylate, $[Ru_2(O_2CMe)_4]_3[Cr(CN)_6]$ (Me = methyl, CH_3) [1–4], or $Cr(Ru_2)_3$ for short, is a highly unusual magnetic material. The dipolar coupling $K_c \approx 5 \times 10^{-3}$ meV between sublattices is more than two orders of magnitude smaller than the coupling $J_c \approx 1.5$ meV between neighboring Ru_2 and Cr ions within each cubic sublattice [5]. Due to the antiferromagnetic intrasublatice coupling J_c, each sublattice orders ferrimagnetically below $T_c \approx 33$ K. At low fields, the two sublattices have opposite moments due to the antiferromagnetic inter-sublattice coupling K_c. They are magnetically aligned by a small field $H_c \sim K_c/\mu_B$ of about 800 Oe [6]. The wide separation of intra- and inter-sublattice couplings is responsible for most of the remarkable properties of this material.

Because of the large vacant space at the center of each cubic unit cell, a single-sublattice compound of $Cr(Ru_2)_3$ is amorphous [3]. Body-centered cubic $Cr(Ru_2)_3$ contains two cubic sublattices, each with lattice constant a. A Cr ion from one sublattice sits at the center of the unit cell of the other. While the $S = 3/2$ Cr(III) ions at the corners of the cubic unit cell for each sublattice do not experience any spin-orbit coupling, the $S = 3/2$ mixed-valent Ru_2(II/III) complex at the middle of each edge experiences the strong crystal field produced by the surrounding Me "paddle-wheel" sketched in Fig.1(b). Consequently, each Ru_2 spin $\mathbf{S}$ is severely constrained by easy-plane anisotropy $D(\mathbf{S}\cdot\mathbf{v})^2$ with $D \approx 100$ K (8.6 meV) [7, 8] and unit vector $\mathbf{v}$ pointing to one of the neighboring Cr ions.

Using simple symmetry arguments, Fishman *et al.* [5] constructed the spin state of each sublattice of $Cr(Ru_2)_3$. For infinite anisotropy and classical spins, the predicted ground state of each sublattice is plotted in Fig.1(a). The Ru_2 spins on the a, b, and c sites lie in the yz, xz, and xy planes. For example, the spin of the Ru_2 complex at the a site $(a/2, 0, 0)$ is $S(0, 1, 1)/\sqrt{2}$, the spin at the b site $(0, a/2, 0)$ is $S(1, 0, 1)/\sqrt{2}$, and the spin at the c site $(0, 0, a/2)$ is $S(1, 1, 0)/\sqrt{2}$. Due to the antiferromagnetic coupling J_c between Ru_2 and neighboring Cr spins, the Cr spin is $-S(1, 1, 1)/\sqrt{3}$ and the net sublattice spin $M_{sl}\mathbf{n}$ lies along $\mathbf{n} = (1, 1, 1)/\sqrt{3}$ with $M_{sl} = (\sqrt{6} - 1)S \approx 2.17$ per $Cr(Ru_2)_3$ unit cell. For finite anisotropy and quantum spins, the Ru_2 spins will cant out of the easy planes towards $\mathbf{n}$, albeit with suppressed amplitudes. Even so, the total spin of each sublattice is predicted to lie along a cubic diagonal.

Keep in mind that another sublattice penetrates the unit cell in Fig.1(a). From the second sublattice, a Cr ion lies at the center of the cube and Ru_2 complexes lie at the middle of each face. Due to the absence of molecular overlap, the interaction between the two sublatices is purely dipolar. At low temperatures, each sublattice is magnetically ordered with spin $M_{sl}\mathbf{n}_1$ or $M_{sl}\mathbf{n}_2$ along one of the 8 cubic diagonals $\pm(1, 1, 1)/\sqrt{3}$, $\pm(-1, 1, 1)/\sqrt{3}$, $\pm(1, -1, 1)/\sqrt{3}$, or $\pm(1, 1, -1)/\sqrt{3}$. Below the critical field H_c, the two sublattice spins are antiferromagnetically aligned with $\mathbf{n}_1 = -\mathbf{n}_2$ and the ground state is 8-fold degenerate. Above H_c, $\mathbf{n}_1$ and $\mathbf{n}_2$ are aligned as close as possible to the external field direction.

Until now there have been no direct measurements of the ground state of $Cr(Ru_2)_3$. Based on neutron-scattering measurements of a deuterated, polycrystalline sample, this paper provides the first direct evidence for the spin state of a single sublattice of $Cr(Ru_2)_3$. In order to place those neutron-scattering results in proper context, we briefly review previous theoretical and experimental work on $Cr(Ru_2)_3$.

The metamagnetic transition at the critical field H_c can be described by a very simple model [5]. With $\mathbf{n}_1$ and $\mathbf{n}_2$ constrained to lie along one of the eight cubic diagonals, the total energy of a magnetic configuration with sublattice orientations $\{\mathbf{n}_{1i}, \mathbf{n}_{2i}\}$ on cluster i in a magnetic field $\mathbf{H} = H\mathbf{m}$ is

$$E = N_{\rm Cr}\sum_i \Big\{-\mu_B M_{sl} H(\mathbf{n}_{1i} + \mathbf{n}_{2i})\cdot\mathbf{m} + K_c {M_{sl}}^2\, \mathbf{n}_{1i}\cdot\mathbf{n}_{2i} - \frac{H^2}{4}\chi_{def}(\mathbf{n}_{1i}, \mathbf{n}_{2i}; \mathbf{m})\Big\}. \quad (1)$$

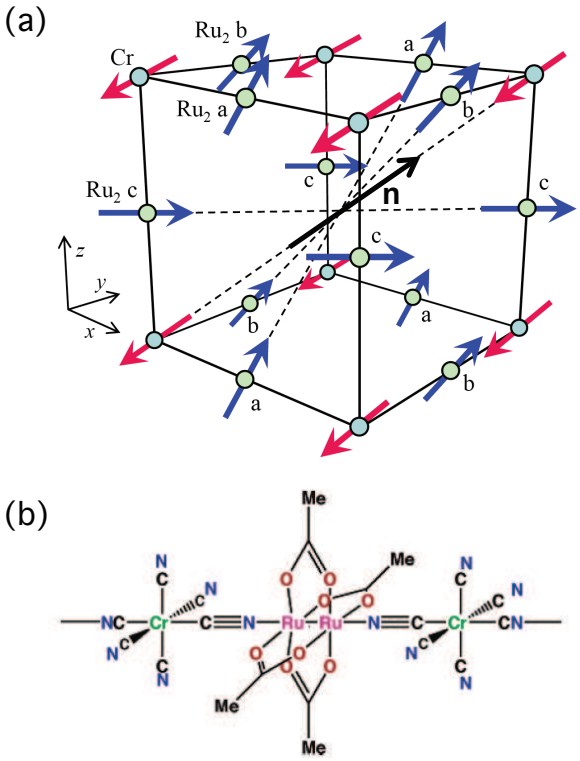

FIG. 1: (a) The predicted ground state [5] of a single sublattice of $Cr(Ru_2)_3$ for infinite anisotropy and classical spins. The net sublattice spin points along $\mathbf{n} = (1,1,1)/\sqrt{3}$ or one of the 8 different cubic diagonals. (b) A sketch of the Ru_2 complex with surrounding Me "paddlewheel."

The parameters in this model are the sublattice spin M_{sl}, the antiferromagnetic exchange K_c between sublattices, the number $N_{\rm Cr}$ of unit cells within a magnetically correlated region ($N_{\rm Cr}/2$ Cr spins belonging to each sublattice), and the susceptibility χ_{def} due to the small deformation of each sublattice spin configuration. Whereas the antiferromagnetic exchange tends to keep the two sublattices antiparallel with $\mathbf{n}_{1i} = -\mathbf{n}_{2i}$, the magnetic field tends to align the two sublattices with $\mathbf{n}_{1i} = \mathbf{n}_{2i}$ as close as possible to the field orientation $\mathbf{m}$.

For each cluster containing $N_{\rm Cr}$ unit cells with sublattice orientations $\mathbf{n}_1$ and $\mathbf{n}_2$, the total magnetization is given by

$$2\mu_B \mathbf{M}_{clust}(\mathbf{n}_1,\mathbf{n}_2;\mathbf{m}) = \mu_B M_{sl} N_{\rm Cr}(\mathbf{n}_1+\mathbf{n}_2) + \frac{N_{\rm Cr}}{2}\chi_{def}(\mathbf{n}_1,\mathbf{n}_2;\mathbf{m})H\mathbf{m}, \quad (2)$$

which contains only the induced change in magnetization parallel to the external field. Because the available samples of $Cr(Ru_2)_3$ are polycrystalline, the magnetization

$$2\mu_B \mathbf{M} = 2\mu_B \sum_i \mathbf{M}_{clust}(\mathbf{n}_{1i},\mathbf{n}_{2i};\mathbf{m}) \quad (3)$$

must be averaged over all field directions $\mathbf{m}$. The average magnetization along the field direction

$$\mu_B M_{av} = 2\mu_B \sum_i \int \frac{d\Omega_{\mathbf{m}}}{4\pi} \langle \mathbf{M}_{clust}(\mathbf{n}_{1i},\mathbf{n}_{2i};\mathbf{m})\rangle \cdot \mathbf{m} \quad (4)$$

contains both an integral over all orientations (with solid angle $\Omega_{\mathbf{m}}$) of the external field and a thermal average over the $8\times 8 = 64$ possible values for $\{\mathbf{n}_{1i},\mathbf{n}_{2i}\}$ within each cluster.

Since the intra-sublattice coupling J_c only enters the energy E implicitly through M_{sl}, the model described above is rather oversimplified. Nevertheless, this model successfully describes $Cr(Ru_2)_3$ due to the wide separation of energy scales. Because the inter-sublattice coupling $K_c \sim 5\times 10^{-3}$ meV is more than two order of magnitude smaller than both $J_c \sim 1$ meV and $D \sim 10$ meV, the magnetic field $H_c \sim K_c/\mu_B$ required to align the two sublattices only weakly perturbs the spin state of each sublattice. Consequently, each sublattce spin state can be treated as nearly "rigid" with net moment confined to one of the cubic diagonals.

The assumption of a rigid sublattice state only fails at high fields and high temperatures, when the "small" deformation term in Eq.(2) becomes comparable to the "rigid" first term [5]. The deformation susceptibility $\chi_{def}(\mathbf{n}_1,\mathbf{n}_2;\mathbf{m})$ in Eqs.(1) and (2) is responsible for both the small linear slope in the average magnetization $M_{av}(T,H)$ at low fields $H \ll H_c$ and for the lack of complete saturation at high fields $H \gg H_c$.

Results for the model parameters based on fits to the experimental values for $M_{av}(T,H)$ were discussed in Ref.[5]. The inter-sublattice coupling K_c involves both the dipolar interaction between "rigid" sublattices, which is ferromagnetic, and the dependence of the sublattice deformation on the relative orientation $\mathbf{n}_1\cdot\mathbf{n}_2$ of the two sublattices, which must then favor antiferromagnetic alignment. According to the fits, K_c increases from 5.2×10^{-3} meV at 5 K to 7.5×10^{-3} meV at 30 K. This rise may be caused by the enhanced deformation of antiferromagnetically aligned sublattices with increasing temperature.

Also based on fitting results, the magnetic correlation length $\xi \sim {N_{\rm Cr}}^{1/3}$ of each sublattice obeys the critical scaling $\xi \propto (1-T/T_c)^{\nu}$ with $\nu \approx 1$. Of more importance for comparison with the neutron-scattering data, low-temperature fits yield the sublattice spin $M_{sl}(T=0) \approx 1.9$, which is slightly smaller than the predicted classical value with infinite anisotropy of 2.17. This result suggests that the sublattice spin state contains significant quantum corrections.

Important clues about the pressure-induced phase transition at 7 kbar [9] are provided by the fitting results [10] for $M_{sl}(T,P)$. Explaining the drop of M_{sl} by about 50% above 7 kbar, the Ru_2 complexes may undergo a high- to low-spin transition ($S = 3/2$ to $1/2$) at 7 kbar. Above 7 kbar, the net moment would then reverse sign and point parallel to the Cr spins.

Indirect support [11] for the predicted spin state of $Cr(Ru_2)_3$ comes from the varying fitting results with the

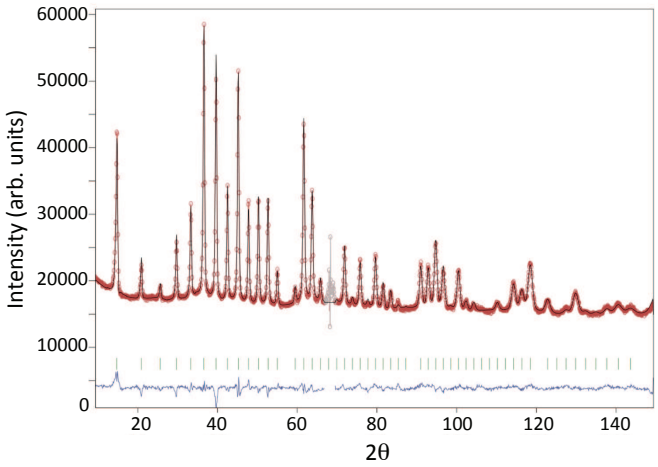

FIG. 2: Diffractogram measured at 50 K. The solid curve is the best fit of the data employing the Rietveld method. The bottom blue curve is the difference between observed and calculated intensities. The green lines indicate the positions of the reflections indexed in $Im\bar{3}m$ with $a = 13.3028(2)$ Å.

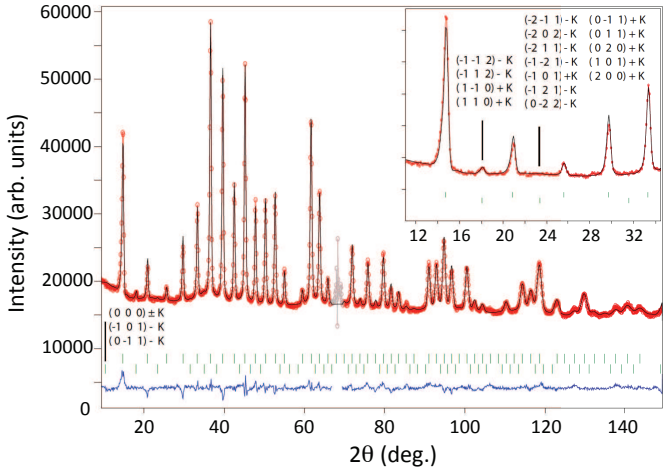

FIG. 3: Diffractogram measured at 1.8 K. The solid curve is the best fit of the data employing the "quantum model" for the magnetic phase. The first row of green lines indicates the positions of the reflections indexed in $Im\bar{3}m$ with $a = 13.291(2)$ Å. The second line indexes the magnetic phase with a PV $K = (0, 0, 1)$, or its equivalents, in the space group $Im\bar{3}m$. The inset enlarges the low-angle portion of the diffractogram, where the small magnetic peak around $2\theta = 18.1^{\circ}$ can be clearly observed. The (h, k, l) indices of three possible magnetic peaks at $2\theta = 10.4^{\circ}$, 18.1°, and 23.4° are indicated.

sublattice spin direction $\mathbf{n}$ confined to (a) cubic diagonals like $(1, 1, 1)/\sqrt{3}$, (b) cubic axis like $(1, 0, 0)$, or (c) face diagonals like $(1, 1, 0)/\sqrt{2}$. Fits obtained under case (a) have values of σ^2 that are 5 and 15 times smaller than for cases (b) and (c), respectively. Hence, the best description for the metamagnetic transition is obtained with the sublattice spins confined to the cubic diagonals.

Local evidence for the predicted sublattice configuration of $Cr(Ru_2)_3$ was provided by a recent muon spin-relaxation study [12]. For every muon site, Lancaster *et al.* calculated the distribution of the dipole fields for each sublattice configuration. Comparing the predicted and experimental results at 1.8 K indicated that the sublattice spins were confined to the cubic diagonals.

Nevertheless, previous evidence for the ground state of $Cr(Ru_2)_3$ can best be described as "circumstantial." We now report the first direct measurement of the $Cr(Ru_2)_3$ spin state using powder neutron diffraction. Structural and magnetic characterizations were made on a deuterated sample of $Cr(Ru_2)_3$ [13]. Experiments were performed in the high-flux and medium-resolution D20 diffractometer at the Institut Laue-Langevin at Grenoble. The D20 instrument is equipped with a PSD-detector spanning an angular range from $2\theta = 1^{\circ}$ to 161° with a wavelength $\lambda = 2.413$ Å. The data were taken after cooling the sample from room temperature to ~ 1.8 K. After warming, neutron powder-diffraction data were collected in the paramagnetic phase at 50 K.

As seen in Fig.2, the diffractogram collected at 50 K can be indexed in the body-centered cubic space group $Im\bar{3}m$ with lattice parameter $a = 13.3028(2)$ Å. An acceptable refinement of the diffractogram was obtained by including two different positions for the deuterium atoms of the methyl groups. One deuterium position is rotated by $n\pi/3$ with respect to the other and the occupancy for every position is exactly $1/2$, which suggests that the deuterium atoms of the methyl group are disordered. This diffractogram also helped us to characterize the disorder of the metal groups.

In order to determine the magnetic structure at 1.8 K, we acquired data over a long 5 hour duration. Together with the paramagnetic diffractogram of Fig.2, the magnetic signal around $2\theta = 18.1^{\circ}$ in the diffractogram plotted in Fig.3 indicates the presence of three-dimensional magnetic order. This peak was indexed using a propagation vector (PV) $K = (0, 0, 1)$ or it equivalents, which implies that the magnetic moments related by the centering translation symmetry operation have opposite sign. Because $K \neq 0$, it was possible to decouple the nuclear and magnetic signals and to refine the structural parameters at low temperature. The lattice parameter at 1.8 K is $a = 13.291(2)$ Å.

It has probably not escaped notice that the intensity of the single magnetic peak at low temperatures is much weaker than that of a typical nuclear peak. Despite this small magnetic intensity, the theory of irreducible representations allows us to identify the magnetic models compatible with the space symmetry. Calculations were aided by the BASIREPS code [14] for $K = (0, 0, 1)$. The decomposition of the magnetic representations for the Cr and Ru sites into irreducible representations is given by $\Gamma_{Cr} = \Gamma^{10}$ and $\Gamma_{Ru} = \Gamma^2 + \Gamma^5 + \Gamma^7 + \Gamma^8 + \Gamma^9 + 2\Gamma^{10}$. Since Γ^{10} is the only irreducible representation that appears for both Cr and Ru, it must describe the magnetic structure of $Cr(Ru_2)_3$ for both the Cr and Ru moments to order at the same temperature. According to Γ^{10}, the two Ru ions

within each Ru_2 complex are coupled ferromagnetically.

The most general magnetic model represented by Γ^{10} has 10 free parameters (6 for the Ru_2 complexes, 3 for the Cr ions, and 1 for the sign of the coupling between the Cr and Ru_2 moments). The models considered in Ref.[5] are a subset of the more general class represented by Γ^{10} in which the moments on the a, b, and c Ru_2 complexes are related by symmetry so that the magnetic structure is invariant under permutation of the a, b, and c labels and the Ru_2 and Cr moments are coupled antiferromagnetically. Consequently, the net Ru_2 moment points along one cubic diagonal and the Cr moment points opposite. These assumptions reduce the number of free parameters from 10 to 3. Before considering the general class of models represented by Γ^{10}, we will determine whether this more restrictive class of models is compatible with the diffraction results.

Three different models for the magnetic structure were considered. In model A, the Ru_2 moments were forced to lie along $(1,1,1)/\sqrt{3}$. In model B, the a, b, and c Ru_2 moments were forced to lie parallel to $(0,1,1)/\sqrt{2}$, $(1,0,1)/\sqrt{2}$, and $(1,1,0)/\sqrt{2}$, respectively. Model C relaxes those constraints by allowing the Ru_2 moments to cant away from the easy planes. Models B and C corrrespond, respectively, to the classical and quantum models described in Ref.[5]. While models A and B have two free parameters corresponding to the amplitudes of the Cr and Ru_2 moments, model C has an additional free parameter correponding to the canting angle of the Ru_2 moments out of the easy plane.

All three models were found to be compatible with the diffraction data. However, the best fit was obtained using model C (the "quantum" model), with fitting results given by the solid line in Fig.3. This fit indicates that the moment of each Ru_2 pair is $2.2 \pm 0.8\mu_B$ (with a spin $S = 1.1$ lower than its classical value of 3/2), canted away from the easy plane by about 5°. The estimated Cr moment of $1.2 \pm 0.7\mu_B$ corresponds to a spin $S = 0.6$, which is much smaller than its classical value of 3/2. The total moment of each sublattice along a cubic diagonal is estimated to be $4.6 \pm 2.8\mu_B$, where the large error bars once again reflect the weak magnetic intensity. Although the estimate for the sublattice spin $M_{sl} = 2.3 \pm 1.4$ is higher than both the classical value of 2.2 and the fitted value of 1.9 obtained from the magnetization curves [5], the error bars associated with the powder-diffraction estimate embrace both of those other values.

This leaves open the question whether any other model represented by Γ^{10} can also fit the diffraction data. We have verified that models with net sublattice moment along a cubic diagonal are the only ones that do *not* produce any measurable magnetic signals at the first and third magnetic peaks ($2\theta = 10.4°$ and 23.4°) but do produce a magnetic signal at $2\theta = 18.1°$. The indices of all three angles are indicated in Fig.3. Due to the high symmetry of the compound, several indices contribute to the same scattering angle. The *absence* of magnetic signals at 10.4° and 23.4° allows us to eliminate any model that has net subalttice moment along the edges $(0,0,1)$ or face diagonals $(1,1,0)/\sqrt{2}$ and confirms that the class of model considered above are the only ones that can describe $Cr(Ru_2)_3$.

The results of this paper for the "quantum" model support earlier predictions [5] for the spin state of $Cr(Ru_2)_3$. In particular, powder neutron-diffraction measurements confirm that the sublattice spins are confined by anisotropy to the cubic diagonals and that the model given by Eq.(1) provides an appropriate description of the metamagnetic transition observed in $Cr(Ru_2)_3$.

Much still remains unknown about $Cr(Ru_2)_3$. Future NMR and magnetic susceptibility measurements may clarify the nature of the pressure-induced transition at 7 kbar [6], testing the prediction of a high- to low-spin transition on the Ru_2 complex [10]. We are confident that future experimental and theoretical work on this remarkable compound will continue to provide new physical insights into the behavior of metamagnetic materials.

Supporting Material and Acknowledgements. The CIF files for $Cr(Ru_2)_3$ at 1.8 and 50 K have been deposited in the Cambridge Crystal Database under CCDC 870671 and 870672. The original magnetization data was collected by Dr. William W. Shum [6]. JC acknowledges ILL for the beam time allocated at the D20 instrument. This research was sponsored by the Division of Materials Science and Engineering of the U.S. Department of Energy (RSF), by the Spanish Ministry of Economy and Competitiveness through grants MAT2011-27233-C02-02 and CSD2007-00010 (JC), and by the U.S. National Science Foundation through grant NSF-11063630 (JSM and TEV) for the chemical synthesis. All authors participated in writing the paper.

[1] Liao, Y, Shum WW and Miller JS 2002 *J. Am. Chem. Soc.* **124** 9336
[2] Vos TE, Liao Y, Shum WW, Her J-H, Stephens PW, Reiff WM and Miller JS, 2004 *J. Am. Chem. Soc.* **126** 11630
[3] Vos TE and Miller JS 2005 *Angew. Chem.* **44** 2416
[4] Miller JS, Vos TE and Shum WW 2005 *Adv. Mat.* **17** 2251
[5] Fishman RS, Okamoto S, Shum WW and Miller JS 2009 *Phys. Rev. B* **80** 064401
[6] Shum WW, Schaller JN and Miller JS 2008 *J. Phys. Chem. C* **112** 7936
[7] Shum WW, Liao Y and Miller JS 2004 *J. Phys. Chem. A* **108** 7460
[8] Miskowiski VM, Hopkins MD, Winkler JR and Gray HB 1999 *Inorganic Electronic Structure and Spectroscopy, Vol. 2*, ed EI Solomon (New York, A.B.P. Lever, John Wiley & Sons) ch 6

[9] Shum WW, Her J-H, Stephens PW, Lee Y and Miller JS 2007 *Adv. Mat.* **19** 2910
[10] Fishman RS, Shum WW and Miller JS 2010 *Phys. Rev. B* **81** 172407
[11] Fishman RS and Miller JS 2011 *Phys. Rev. B* **83** 094433
[12] Lancaster T, Pratt FL, Blundell SJ, Steele AJ, Baker PJ, Wright JD, Watanabe I, Fishman RS and Miller JS 2011 *Phys. Rev. B* **84** 092405
[13] Prepared by the method described in Ref.[2], using acetic acid-d_4, and acetic anhydride-d_6.
[14] Rodrguez-Carvajal J 1993 *Physica* **B192** 55. Programs of the FullProf Suite and their corresponding documentation can be obtained at http://www.ill.eu/sites/fullprof/.